

Chaos and the Flow Capture Problem: Polluting is Easy, Cleaning is Hard


Lachlan D. Smith,^{1,*}† Guy Metcalfe,² and Julio M. Ottino^{1,3,4}

¹Department of Chemical and Biological Engineering, Northwestern University, Evanston, Illinois 60208, USA

²Department of Mechanical and Product Design Engineering, Swinburne University of Technology, Hawthorn, Victoria 3122, Australia

³Department of Mechanical Engineering, Northwestern University, Evanston, Illinois 60208, USA

⁴The Northwestern Institute on Complex Systems (NICO), Northwestern University, Evanston, Illinois 60208, USA

 (Received 8 March 2018; revised manuscript received 9 July 2018; published 25 September 2018)

Cleaning pollution from a heterogeneous flow environment is far from simple. We consider the flow capture problem, which has flows and sinks in a heterogeneous environment, and investigate the problem of positioning pollutant capture units. We show that arrays of capture units carry a high risk of failure without accounting for environmental heterogeneity and chaos in their placement, design, and operation. Our idealized two-dimensional models reveal salient features of the problem. Maximum capture efficiency depends on the required capture rate: long-term efficiency decreases as the number of capture units increases, whereas short-term efficiency increases. If efficiency is important, the capture process should begin as early as feasible. Knowledge of transport controlling flow structures offers predictability for unit placement. We demonstrate two heuristic approaches to near-optimally position capture units.

DOI: [10.1103/PhysRevApplied.10.034055](https://doi.org/10.1103/PhysRevApplied.10.034055)

I. INTRODUCTION

Consider the problem of positioning units in a heterogeneous flow environment to capture something moved by the flow through the environment. We label this the *flow capture problem*, which has many applications. For example, in the ocean mussels massively congregate on the pilings of wind farms. An unintended consequence of this buildup is that a large portion of phytoplankton is filtered out of the surrounding water, leading to substantial change in local ocean ecology [1]. Another example is removal of a pollutant from an environment, e.g., microplastics that are accumulating in oceans and waterways [2,3] or capturing CO₂ directly from the atmosphere in an effort to limit global temperature rise [4–8]. The central question in all these examples is as follows: Where should capturing units be placed in order to meet specified objectives, e.g., minimizing the impact of mussel congregation or maximizing pollutant removal? All these cases are specific examples of the flow capture problem, problems involving flows and sinks. The most challenging capture problems involve complex flows.

The flow capture problem can be cast in two ways. The first maximizes the total amount of captured material after some fixed length of time. This setting resembles

facility location optimization problems [9], for example, sensor placement in water or ventilation distribution systems to detect a maliciously injected contaminant [10] or in cell-phone contact networks to detect a virus [11], problems, in principle, solvable using large-scale mixed-integer linear programming. But there are several things that make the general flow capture problem more challenging. The shapes of the captured regions can, in general, be very complex, possibly fractal, and need not be convex or simply connected (they have holes). Moreover, finding the region that is captured by a unit is difficult. The second type of flow capture problem optimizes unit placement to minimize the time to reach a critical value of capture (maximizing the capture rate). This problem accounts for time-dependent capture, i.e., the capture zone for a unit increases as a function of time and cannot easily be cast as a facility optimization problem. The capture rate can also be understood by considering capture units as the leaks in leaking chaotic systems [12]. Over long times, the capture rate decays exponentially at a predictable rate. However, over short times, the capture rate is much less predictable and is highly sensitive to a unit's location.

We consider the placement of perfect capture units in three scenarios and estimate how effective cleaning will be in each case.

1. Steady homogeneous flow. No chaos; just uniform, unidirectional flow.

*lachlan.smith@sydney.edu.au

†Present address: School of Mathematics and Statistics, The University of Sydney, Sydney, NSW 2006, Australia

2. Complex heterogeneous flow, but we assume no knowledge of the flow, i.e., placement choice is blind to local flow heterogeneity;

3. Complex heterogeneous flow, but we use knowledge of the flow to inform placement.

Define $P(t)$ as the fraction of pollutant concentration in the domain at time t and assume an initially uniform concentration: $P(t=0) = 1$. Define P_c as the target value of P that we want to reduce to. The effectiveness of N removal units is determined by whether or not they can reduce P to less than P_c in finite time: $P \leq P_c$ defines success, while $P > P_c$ for all t is failure.

II. UNIFORM FLOW

First consider steady flow on a doubly periodic square domain of side length h . For each fixed number of units N , each unit interacts with only a small fixed swathe of the domain: P decreases linearly from 1, levels out to some value, and stays there for all time. Once a unit's swathe is exhausted of pollutant, no new pollutant ever comes to that unit. Each unit captures an area equal to δh , where δ is the unit characteristic capture size. Therefore, the equilibrium value of P is $1 - N\delta/h$, assuming the units do not overlap. As N grows, the equilibrium value of P decreases. For $N \geq N_c = (h/\delta)(1 - P_c)$, P will be lower than P_c and cleaning will be successful. We can define a long-time measure of effectiveness for the steady flow as

$$E(N) = \begin{cases} 0 & \text{for } N \text{ such that } P > P_c, \\ 1 & \text{for } N \text{ such that } P \leq P_c, \end{cases} \quad (1)$$

and $E(N) = 0$ for $N < N_c$, $E(N) = 1$ for $N \geq N_c$.

III. EFFECTIVENESS OF RANDOM PLACEMENT IN COMPLEX FLOWS

What about complex two-dimensional flows, with non-mixing islands interspersed amongst a chaotic sea? We first pretend we know nothing about the underlying flow, but we can measure $P(t)$. We consider the double-gyre flow [13], a model for two gyre systems observed in geophysical flows, in three representative cases. The time-periodic velocity is given by

$$\begin{aligned} v_x(x, y, t) &= -\frac{\pi}{2} \sin[\pi f(x, t)] \cos(\pi y), \\ v_y(x, y, t) &= \frac{\pi}{2} \cos[\pi f(x, t)] \sin(\pi y) \frac{\partial f}{\partial x}(x, t), \\ f(x, t) &= \epsilon \sin(2\pi t)x^2 + [1 - 2\epsilon \sin(2\pi t)]x, \end{aligned} \quad (2)$$

with time period equal to 1. For $\epsilon = 0.01$, the flow is mostly nonchaotic, as shown by the Poincaré section [14] (red) in Fig. 1(a), which is dominated by two nonmixing

islands. We label this case nonchaotic. For $\epsilon = 0.05$, the chaotic sea has approximately the same area as the nonchaotic islands, as shown in Fig. 1(b), and we label this case mixed. Lastly, for $\epsilon = 0.25$, the flow is fully chaotic, evidenced by the lack of islands in Fig. 1(c). We label this case chaotic. In each figure of Fig. 1, the circles are $J = 50$ capture units (sinks) of equal diameter $\delta = 0.1$ (the shading is explained later). Here we only consider combinations of these 50 locations; however, the complete

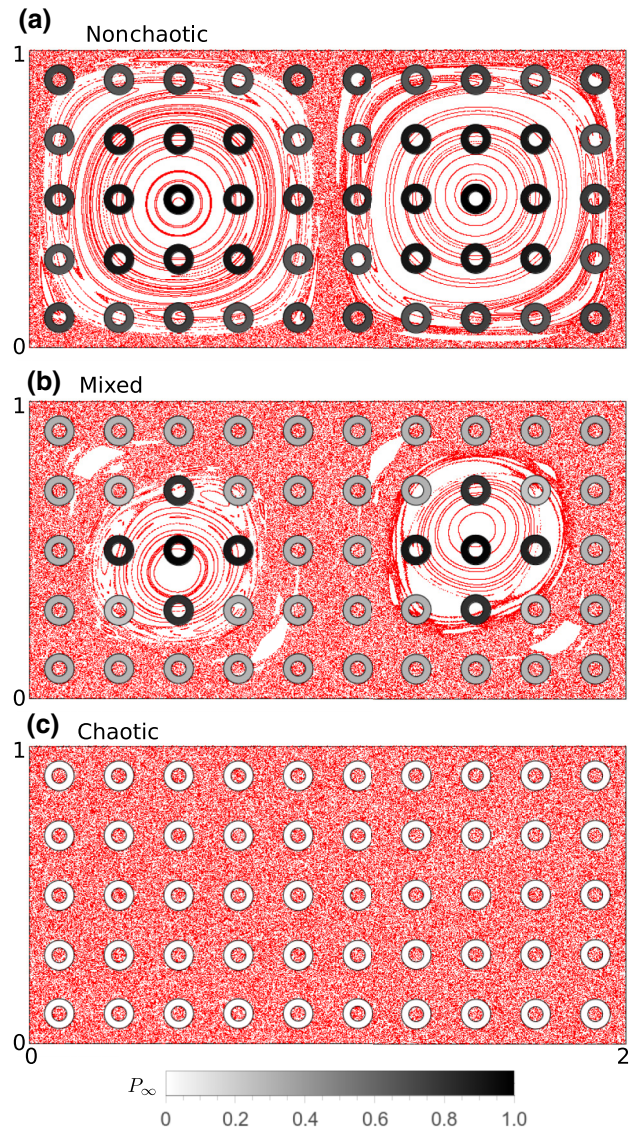


FIG. 1. Poincaré sections (red) generated by the double-gyre flow Eq. (2) for (a) $\epsilon = 0.01$, which is mostly nonchaotic, (b) $\epsilon = 0.05$, which has approximately equal areas of chaotic and nonchaotic regions, and (c) $\epsilon = 0.25$, which is fully chaotic. The circles, of diameter $\delta = 0.1$, are possible sites for capture units, which are colored according to P_∞ for each unit run in isolation, i.e., $N = 1$. No pollutant removal means $P_\infty = 1$, shown as black, and total removal means $P_\infty = 0$, shown as white, which is achieved by all locations in (c).

flow capture problem allows each site to be located *anywhere* in the domain. Any pollutant that reaches a sink is immediately removed from the domain. For each value of N and each flow case, we measure $P(t)$ for all combinations of N units from the grid of possible sites shown in Fig. 1, to obtain ensemble statistics. Note the explosion of possible site combinations. Even for our simple example with just 50 possible sites, for $N = 5$ there are over two million possible combinations. Moreover, the reality is that we would not be able to build N sites, only to tear them down and build them afresh until we discovered the optimum placement. We get only one pass through the distribution of possible outcomes.

Figure 2 shows the ensemble averages of $P(t)$ for the three cases; however, the averages hide as much as they reveal. As N increases, more pollutant is removed on average, but for each N , the long-time value of P , P_∞ [15], for each combination of sites can diverge strongly from the average. Some site combinations achieve values of P_∞ much lower than P_c , or reach P_c very quickly, while other combinations never reach P_c . Like Eq. (1), we define a long-time effectiveness for each combination of N sites, (m_1, \dots, m_N) , as

$$E(m_1, \dots, m_N) = \begin{cases} 0 & \text{if } P_\infty > P_c, \\ 1 & \text{if } P_\infty \leq P_c, \end{cases} \quad (3)$$

and plot the probability that a random combination of N sites will be effective, $\mathbb{P}[E = 1]$, in Fig. 3. For the nonchaotic case [Fig. 3(a)], not surprisingly, when N and P_c are small, few combinations of sites will be effective, while for large N most combinations will be effective. For instance, for $N = 1$, no individual site is capable of reaching $P_c \leq 0.6$, whereas almost all combinations of five sites achieve $P_c = 0.6$. Note that for $N = 5$, no combination is able to achieve $P_c \leq 0.2$.

In stark contrast, in the fully chaotic case [Fig. 3(c)], *every* individual site cleans the entire domain, meaning $\mathbb{P}[E = 1] = 1$ for every value of P_c . This is because dynamics in the chaotic region are ergodic, i.e., trajectories of tracer particles densely fill the chaotic region. Therefore, every pollutant particle will eventually be captured, regardless of the position of the capture unit. This shows that the biggest challenge to long-term removal is the presence of nonchaotic regions. However, for shorter time frames, the capture sites in the chaotic case do not clean the entire domain and some sites capture more than others. This means optimal siting is important if cleaning must occur rapidly.

The mixed case [Fig. 3(b)] falls in between the two extremes. Single units ($N = 1$) are not able to clean the entire domain, but they are able to achieve smaller values of P_c than the nonchaotic case. Note that even when $N = 5$, no combination can clean the entire domain. This is linked to the size of the two nonchaotic islands, which

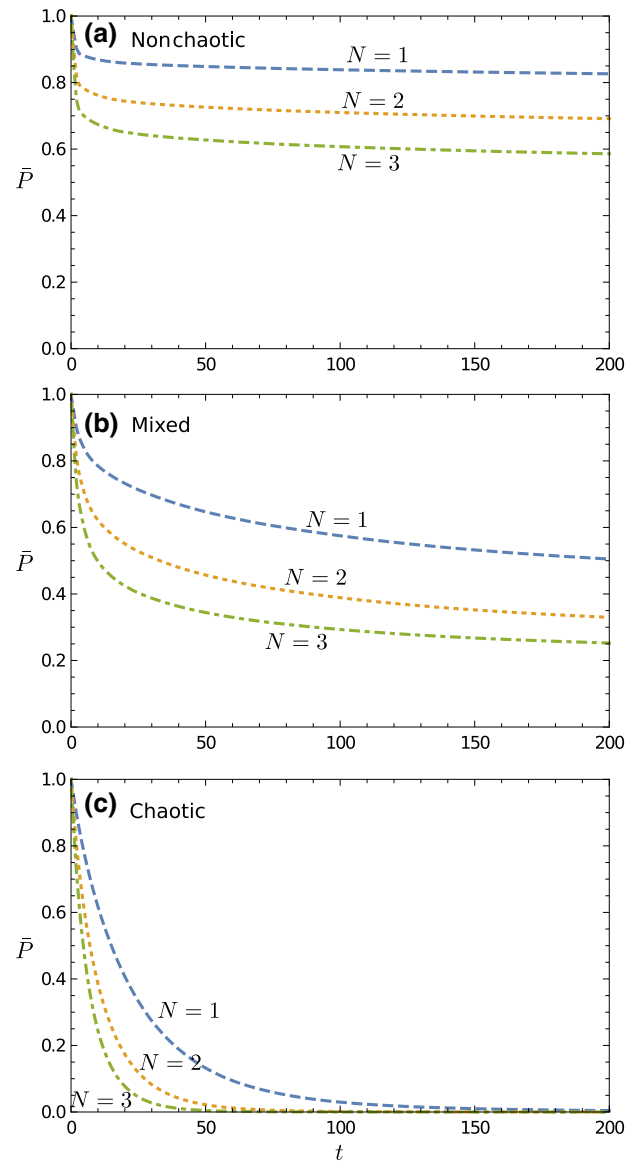


FIG. 2. Averages of $P(t)$ over all combinations of N sites from the grid in Fig. 1, for $N = 1, 2$, and 3 , and the three cases shown in Fig. 1, (a) nonchaotic, (b) mixed, and (c) chaotic. As we choose N sites from $J = 50$ possible sites, the number of possible combinations grows as the binomial coefficient, rising rapidly from 50 combinations for $N = 1$ to over two million for $N = 5$.

have diameter slightly greater than five times the diameter of the capture unit.

For the nonchaotic and mixed cases, failure occurs even though our model capture units are assumed perfect at cleaning the fluid they receive. Failure is entirely a function of the heterogeneity of the environment, in particular, nonchaotic islands. The clear message is that for all but fully chaotic flows, the more ambitious the pollution reduction target, the more dominant the consideration of site location becomes.

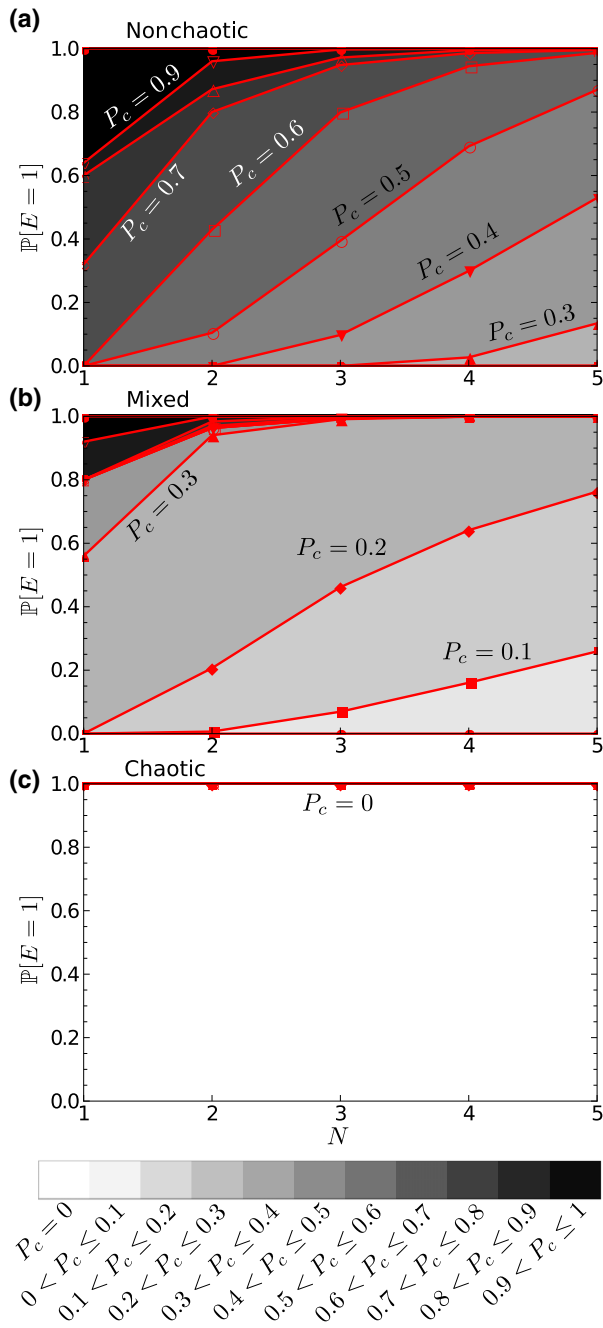


FIG. 3. Probability of success of a random combination of N sites, i.e., probability that the combination will achieve $E = 1$ from Eq. (3), for each of the three cases, (a) nonchaotic, (b) mixed, and (c) chaotic. Each red curve corresponds to a different value of P_c , ranging from 0 to 1 in increments of 0.1.

IV. INFORMED PLACEMENT BASED ON FLOW CHARACTERISTICS

A. Maximum capture efficiency

On the other hand, what if we do know the Lagrangian characteristics of the flow? Now we can choose the most efficient combination of N sites, i.e., those that remove the

most pollutant after a long time, or those that reach the target P_c the fastest. There are several ways to define efficiency. We can define the efficiency of a set of N units as the total amount captured divided by N , i.e.,

$$\eta(m_1, \dots, m_N) = \frac{1 - P_\infty}{N}, \quad (4)$$

which is the average removal per unit. Figure 4 shows that in all three cases (nonchaotic, mixed, and chaotic), as N increases, the maximum η efficiency (blue triangles, left vertical axis) decreases. This is because the regions cleaned by different units overlap, and there is generally more overlap when more units are used. In the facility location problem this diminishing returns property is called submodularity. For general flows with chaotic and regular regions, overlapping capture regions will be unavoidable, even when the best combination of unit locations is chosen.

We can also define the efficiency of a set of N units as the rate at which they approach success (reach P_c) by

$$\zeta(m_1, \dots, m_N) = \frac{1 - P_c}{N\tau}, \quad (5)$$

where τ is the time required to reach P_c . Equation (5) measures the rate efficiency of the capture process, whereas Eq. (4) measures total long-time efficiency. Unlike the maximum η efficiency, the maximum ζ efficiency does not suffer from diminishing returns, as shown by the red circles and squares in Fig. 4. In all cases shown in Fig. 4, the maximum ζ efficiency initially increases with N . This means that using more units is more efficient for short-term goals, but in the long term fewer units is more efficient. For example, an increase in ζ from $N = 1$ to $N = 2$, as occurs in the mixed and chaotic cases [Figs. 4(b) and 4(c)], means the rate of capture more than doubles when the number of units is doubled. However, in the mixed case with $P_c = 0.5$, and the two chaotic cases, ζ does not increase monotonically. This suggests that there is an optimal choice of N at which peak ζ efficiency is achieved, e.g., $N = 4$ in the mixed case with $P_c = 0.5$.

B. Heuristic methods to find near-optimal site locations

Another important question is how to choose the most effective N sites based *only* on characteristics of the flow, rather than measuring P_∞ for all possible site combinations? At short times, pollutant captured by a unit is proportional to the total volume of fluid that passes through it. Therefore, the best short-term results are obtained by locating units in regions with high velocity. However, at long times, the total volume of fluid that passes through a unit is not a good predictor of performance, because clean fluid may continually recycle through units.

For time-periodic flows, such as the double-gyre example considered here, we can predict the long-term

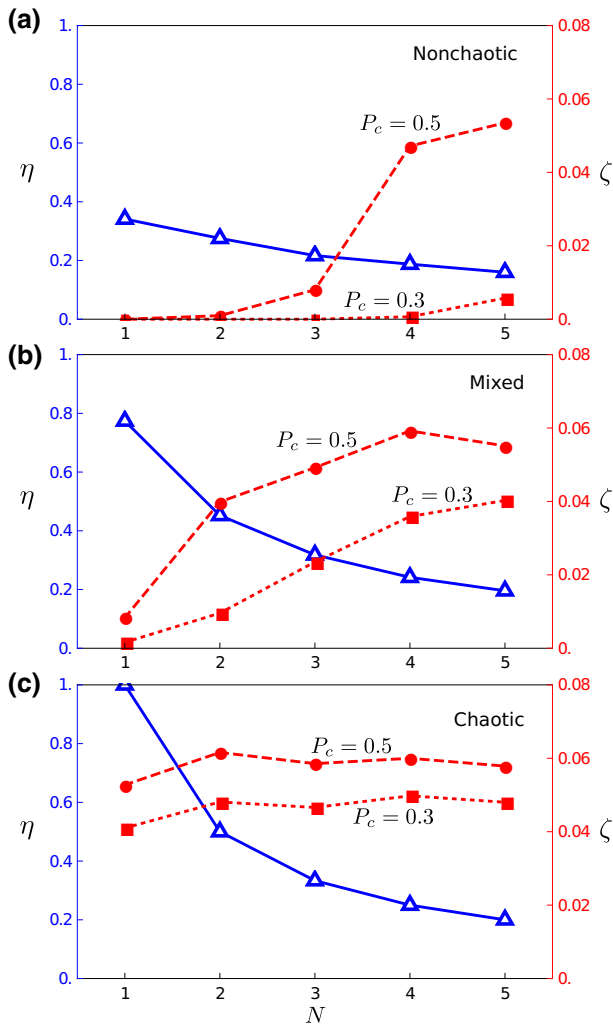


FIG. 4. Efficiency measures for N capturing units in each of the three cases, (a) nonchaotic, (b) mixed, and (c) chaotic. Maximum η efficiency of N units [Eq. (4)] is shown as blue triangles, solid connecting lines on the left vertical axis. Maximum ζ efficiency of N units [Eq. (5)] for $P_c = 0.5$ (red circles, dashed) and $P_c = 0.3$ (red squares, dotted) on the right vertical axis.

performance of any proposed site using flow properties. The captured region is the infinite-time streak surface that emanates from a unit m , which can be written as the set

$$C(m) = \bigcup_{n=0}^{\infty} T^n S(m), \quad (6)$$

where T is the map that takes a particle to its position after one flow period, and $S(m)$ is the set of streak trajectories emanating from a unit over one flow period: $C(m)$ is the union of all chaotic and coherent regions (invariant tori) that intersect $S(m)$. Importantly, $C(m)$ contains the entire chaotic region if and only if $S(m)$ intersects some portion of the chaotic region [16]. Two examples are shown in Fig. 5. For the unit m_1 (dark blue circle), $S(m_1)$ (dark

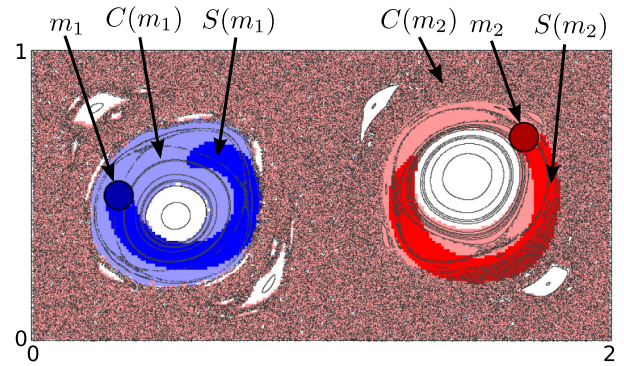


FIG. 5. The captured region $C(m)$ (light blue and light red) for two intake units, $m = m_1$ (blue circle) and $m = m_2$ (red circle). $C(m)$ is the infinite-time streak surface emanating from the unit, which is equivalent to the union of iterates of $S(m)$ [Eq. (6)], the set of streak trajectories emanating from the unit over one flow period (dark blue and dark red). For m_1 , $S(m_1)$ intersects coherent regions in the left island, so $C(m_1)$ contains a portion of the left island. However, $S(m_1)$ does not intersect the chaotic region, so it is not captured. For m_2 , $S(m_2)$ intersects coherent regions in the right island: $C(m_2)$ contains a portion of the right island. As $S(m_2)$ also intersects a portion of the chaotic region, the entire chaotic region is contained in $C(m_2)$, even though m_2 is inside the right island.

blue) intersects invariant tori in the left island, so $C(m_1)$ (light blue) contains all those invariant tori, i.e., it contains a portion of the left island. However, $S(m_1)$ does not intersect the chaotic region, so it is not captured. For the capture unit m_2 (dark red circle), $S(m_2)$ (dark red) intersects some invariant tori in the right island, so $C(m_2)$ (light red) contains all those invariant tori, i.e., it contains a portion of the right island. $S(m_2)$ also intersects the chaotic region, so $C(m_2)$ contains the entire chaotic region, even though m_2 itself is contained within the right island. There are also coherent regions uncaptured by either unit.

Based on Eq. (6), a good individual site is one such that $S(m)$ intersects a portion of the chaotic region and a collection of coherent regions with a large area. For $N \geq 2$, the best combination of sites is not the same as choosing the best N individual sites, as they may capture the same region. For increasing N , predicting the best sites becomes an increasingly difficult optimization problem. One heuristic approach, which uses the Poincaré section and Eq. (6), is to choose a first site M_1 such that $S(M_1)$ intersects a portion of the chaotic region and the collection of coherent regions with the largest area. The site M_1 captures the entire chaotic region and some coherent regions. For example, the site m_2 in Fig. 5 is a good candidate. Next, choose a site M_2 such that $S(M_2)$ intersects coherent regions with the largest area, excluding the coherent regions that are intersected by $S(M_1)$. For example, the site m_1 in Fig. 5 is a good candidate for the second site because $S(m_1)$ intersects the outer edge of the left island,

Algorithm I. Choose N sites based on qualitative properties of the Poincaré section and Eq. (6)

-
- 1: Generate the Poincaré section
 - 2: Choose the first site, M_1 such that $S(M_1)$ intersects the chaotic region and invariant tori whose union has the largest area
 - 3: **for** $i = 2, \dots, N$ **do**
 - 4: Choose site location M_i such that $S(M_i)$ intersects invariant tori whose union has the largest area, excluding invariant tori intersected by $S(M_1), \dots, S(M_{i-1})$
 - 5: **end for**
 - 6: **return** Sites M_1, \dots, M_N
-

which is not captured by m_2 . Continue choosing sites M_i such that $S(M_i)$ intersects coherent regions with the largest area that are not captured by the sites M_1, \dots, M_{i-1} . This procedure is summarized in Algorithm I. Note that a computationally simpler approach is to replace the sets $S(M_i)$ in the algorithm with the sets M_i , since M_i is necessarily contained in $S(M_i)$. This alternative approach requires only the Poincaré section to be computed, and not the sets $S(M_i)$. However, the locations chosen will perform worse than if the sets $S(M_i)$ are used.

Consider a second heuristic approach. First, choose the best individual site, M_1 , that minimizes P_∞ . Equivalently, M_1 maximizes the captured area, $C(M_1)$. Then choose a next site, M_2 , such that the pair maximizes the captured area, $C(M_1) \cup C(M_2)$. Continue choosing sites M_i that maximize the captured area, $\bigcup_{j=1}^i C(M_j)$, until N or the capture target, P_c , is reached. This procedure is summarized in Algorithm II. Due to submodularity of η , the amount of pollutant removed using this algorithm will always be within a constant factor of the optimal solution [17]. Figure 6 shows the effectiveness of Algorithm II for the nonchaotic and mixed cases. The global optima for P_∞ (shown as red triangles), found by minimizing P_∞ over all combinations of N locations, are only slightly less than the values obtained from the heuristic approach (shown as black squares). Comparing the computational expense of the two methods, for the global optima, the number of combinations with $J = 50$ possible site locations grows as the binomial coefficient, whereas the heuristic approach requires only JN evaluations. For $N = 5$, this is the difference between over two million evaluations versus 250 evaluations.

Algorithm II. Choose N sites by computing capture regions

-
- 1: Choose J potential site locations, M_1, \dots, M_J , e.g., on a grid
 - 2: Compute the captured region, $C(M_i)$, for each site using particle tracking or Eq. (6)
 - 3: **for** $i = 1, \dots, N$ **do**
 - 4: Choose site location M_i such that $\bigcup_{j=1}^i C(M_j)$ has the largest area.
 - 5: **end for**
 - 6: **return** Sites M_1, \dots, M_N
-

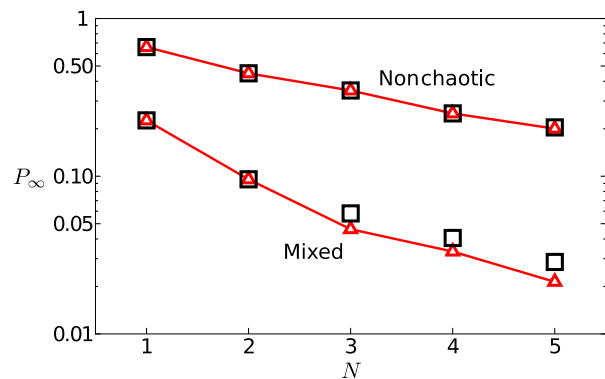


FIG. 6. Minimum P_∞ over all combinations of N units (red triangles) and P_∞ obtained from the heuristic approach described in Algorithm II (black squares). Shown for the nonchaotic (upper) and mixed (lower) cases.

The heuristic algorithms described above do not account for mixing rate and optimizing ζ is, in general, more difficult because it is not submodular (it does not decrease monotonically with N). More sophisticated mathematical techniques could be useful for different applications of the capture problem.

V. CONCLUSIONS

Capturing pollutants from a heterogenous flow environment is far from simple. As our example problem is highly stylized (perfect capture units in a relatively simple time-periodic flow), the absolute numbers from our calculations are not the main point. The important features of the flow capture problem illustrated here are the trends that we expect to persist in more realistic models and across various applications. For example, we see the same trends and qualitative results when the double-gyre flow is replaced with the egg-beater flow [18], which uses periodic boundary conditions (see Supplemental Material [19]). The similarities between our results for the double-gyre flow and the egg-beater flow show that the geometry of transport structures (e.g., islands and the chaotic sea) plays a more important role for the flow capture problem than the specifics (e.g., boundary conditions) of the flows that generate them.

When flow heterogeneity is accounted for, the maximum capture efficiency depends on the required capture rate. Fast capture rates require more units, but over long times, fewer units are more efficient. If efficiency—often related to cost—is important, the removal process should begin as early as feasible.

Dynamical systems (or Lagrangian coherent structures in aperiodic flows) offer a path to predictability for capture unit placement because streak surfaces (manifolds) shape transport in flows [20]. We demonstrate two heuristic algorithms to near-optimally position capture units.

Both algorithms significantly reduce the computational cost of optimization compared to checking all possible combinations of locations. Most importantly, for flows with transport barriers (e.g., islands), placing units in random locations without accounting for the heterogeneity and chaos in the flow carries a remarkably high risk of failure. Even when units capture perfectly, as we assume, or they receive large flow volumes, they may not be effective without accounting for local heterogeneity and chaos in placement, design, and operation.

For fully chaotic flows, single capture units positioned arbitrarily will eventually capture *all* the pollutant. Hence, for long-term capture, there is *no* benefit in optimizing unit location. However, the rate of capture depends on unit location, so some locations are better than others for reaching goals rapidly. We have not explored this dependence in detail here, and it is an important direction for future study. In addition, since every capture unit location will eventually capture all the pollutant, it would seem that there is no benefit to using multiple capture units. However, we have shown that using two units can more than double the rate of capture. Therefore, there can be benefits to using multiple capture units, especially if capture must occur within a specified time.

Future work should explore more complex models, with more realistic velocity fields derived for specific applications, such as microplastic capture in the ocean [2,3] and direct capture of CO₂ from the atmosphere [4–7]. In addition, the effects of turbulent diffusion [21,22], heterogeneous initial pollutant distributions, or pollutant sources in addition to sinks [23] should also be considered. Furthermore, flow capture applications where the pollutant is not a passive tracer pose additional challenges, e.g., capturing inertial microplastic particles [2,3] or motile particles [24–26]. Insights into the general flow capture problem could also be gained by using quantitative Poincaré recurrence theory [27] to analyze removal rates and recirculation rates of capture units in heterogeneous flows.

-
- [1] K. Slavik, C. Lemmen, W. Zhang, O. Kerimoglu, K. Klingbeil, and K. Wirtz, The large-scale impact of offshore wind farm structures on pelagic primary productivity in the southern North Sea, *Hydrobiologia* (2018).
- [2] A. L. Andrady, Microplastics in the marine environment, *Mar. Pollut. Bull.* **62**, 1596 (2011).
- [3] A. Cózar, F. Echevarría, J. I. González-Gordillo, X. Irigoien, B. Úbeda, S. Hernández-León, Á. T. Palma, S. Navarro, J. García-de Lomas, A. Ruiz, M. L. Fernández-de Puelles, and C. M. Duarte, Plastic debris in the open ocean, *Proc. Natl Acad. Sci. USA* **111**, 10239 (2014).
- [4] R. Socolow, M. Desmond, R. Aines, J. Blackstock, O. Bolland, T. Kaarsberg, N. Lewis, M. Mazzotti, A. Pfeffer, K. Sawyer, J. Sirola, B. Smit, and J. Wilcox, Direct air capture

of CO₂ with chemicals: A technology assessment for the APS Panel on Public Affairs, tech. rep., American Physical Society, 2011.

- [5] Core Writing Team, Rajendra K. Pachauri, and Leo Meyer (eds.), IPCC, 2014: Climate Change 2014: Synthesis Report. Contribution of Working Groups I, II and III to the Fifth Assessment Report of the Intergovernmental Panel on Climate Change, tech. rep., 2014.
- [6] P. Smith, S. J. Davis, F. Creutzig, S. Fuss, J. Minx, B. Gabrielle, E. Kato, R. B. Jackson, A. Cowie, E. Kriegler, D. P. van Vuuren, J. Rogelj, P. Ciais, J. Milne, J. G. Canadell, D. McCollum, G. Peters, R. Andrew, V. Krey, G. Shrestha, P. Friedlingstein, T. Gasser, A. Grübler, W. K. Heidug, M. Jonas, C. D. Jones, F. Kraxner, E. Littleton, J. Lowe, J. R. Moreira, N. Nakicenovic, M. Obersteiner, A. Patwardhan, M. Rogner, E. Rubin, A. Sharifi, A. Torvanger, Y. Yamagata, J. Edmonds, and C. Yongsung, Biophysical and economic limits to negative CO₂ emissions, *Nat. Clim. Change* **6**, 42 (2016).
- [7] D. W. Keith, G. Holmes, D. S. Angelo, and K. Heidel, A process for capturing CO₂ from the atmosphere, *Joule* **2**, 8 (2018).
- [8] A. Azapagic, D. Beerling, C. Cheeseman, G. Henderson, C. Hepburn, J. House, C. Le Quere, N. Markusson, N. Shah, J. Shepherd, and P. Smith, Greenhouse gas removal, Technical Report, The Royal Society and the Royal Academy of Engineering, 2018.
- [9] M. Bansal and K. Kianfar, Planar maximum coverage location problem with partial coverage and rectangular demand and service zones, *INFORMS J. Comput.* **29**, 152 (2017).
- [10] A. Krause, J. Leskovec, C. Guestrin, and J. VanBriesen, Efficient sensor placement optimization for securing large water distribution networks, *J. Water Res. Plan. Manage.* **134**, 516 (2008).
- [11] J. Lee, J. J. Hasenbein, and D. P. Morton, Optimization of stochastic virus detection in contact networks, *Oper. Res. Lett.* **43**, 59 (2015).
- [12] E. G. Altmann, J. S. E. Portela, and T. Tél, Leaking chaotic systems, *Rev. Mod. Phys.* **85**, 869 (2013).
- [13] S. C. Shadden, F. Lekien, and J. E. Marsden, Definition and properties of Lagrangian coherent structures from finite-time Lyapunov exponents in two-dimensional aperiodic flows, *Physica D* **212**, 3 (2005).
- [14] The positions of a number of tracer particles are marked at the end of each flow period.
- [15] We use $P(1000)$ to approximate P_∞ , i.e., 1000 flow periods.
- [16] Technically, $C(m)$ contains the entire chaotic region except a set of measure zero, known as the unstable manifold of the chaotic saddle, and the area of the captured region converges asymptotically as $n \rightarrow \infty$ [12].
- [17] S. Fujishige, *Submodular Functions and Optimization* (Elsevier, Amsterdam, 2005).
- [18] J. G. Franjione and J. M. Ottino, Symmetry concepts for the geometric analysis of mixing flows, *Philos. Trans. R. Soc. A* **338**, 301 (1992).
- [19] See Supplemental Material at <http://link.aps.org/supplemental/10.1103/PhysRevApplied.10.034055> for details of the flow capture problem in the egg-beater flow.

- [20] S. Wiggins, *Introduction to Applied Nonlinear Dynamical Systems and Chaos* (Springer-Verlag, New York, 2003).
- [21] D. Lester, M. Rudman, and G. Metcalfe, Low Reynolds number scalar transport enhancement in viscous and non-Newtonian fluids, *Int. J. Heat Mass Transfer* **52**, 655 (2009).
- [22] C. P. Schlick, I. C. Christov, P. B. Umbanhowar, J. M. Ottino, and R. M. Lueptow, A mapping method for distributive mixing with diffusion: Interplay between chaos and diffusion in time-periodic sine flow, *Phys. Fluids* **25**, 052102 (2013).
- [23] J.-L. Thiffeault and G. A. Pavliotis, Optimizing the source distribution in fluid mixing, *Physica D* **237**, 918 (2008).
- [24] T. J. Pedley and J. O. Kessler, Hydrodynamic phenomena in suspensions of swimming microorganisms, *Annu. Rev. Fluid Mech.* **24**, 313 (1992).
- [25] C. Torney and Z. Neufeld, Transport and Aggregation of Self-Propelled Particles in Fluid Flows, *Phys. Rev. Lett.* **99**, 078101 (2007).
- [26] N. Khurana, J. Blawdziewicz, and N. T. Ouellette, Reduced Transport of Swimming Particles in Chaotic Flow due to Hydrodynamic Trapping, *Phys. Rev. Lett.* **106**, 198104 (2011).
- [27] B. Saussol, An introduction to quantitative Poincaré recurrence in dynamical systems, *Rev. Math. Phys.* **21**, 949 (2009).